INPUT-OUTPUT FEEDBACK LINEARIZATION ASSOCIATES WITH LINEAR QUADRATIC REGULATOR FOR STABILIZATION CONTROL OF FURUTA PENDULUM SYSTEM

Thi-Thanh-Hoang Le

Ho Chi Minh city University of Technology and Education (HCMUTE)
01-Vo Van Ngan street, Ho Chi Minh city, Vietnam
***** Corresponding author. E-mail: hoangltt@hcmute.edu.vn

Abstract: Manuscript provides a key technology, namely Input-Output Feedback Linearization Associates with Linear Quadratic Regulator (for short, IOFLALQR). The objective of this research is to study the possibility of integrating two control strategies, which includes input-output feedback linearization technique (for short, IOFL) and linear quadratic regulator controller (for short, LQR), for stabilization control of Furuta pendulum system. Furuta pendulum system belongs to the group of under-actuated robot systems. In this work, structure of IOFLALQR, control implementation, comparison of IOFLALQR and conventional LQR are adequately studied and discussed. Simulation is completed in MATLAB/Simulink environment and experiment is done on real-time experimental setup. Numerical simulation and experimental results show that the IOFLALQR are implemented on Furuta pendulum successfully. Besides, results have been drawn for demonstrating IOFLALQR better than another classical method.

Keywords: Input-output feedback linearization technique; Furuta pendulum; Linear quadratic regulator; Hybrid control; LQR control.

1. Introduction

Main purpose of combination two or three control strategies is to validate ability of integrating those techniques together for stabilization control, swing-up control and more. Many researches have been completed and shown to scientific community related to topic of combining control approaches. Diversity of combination of controllers have been presented such as a combination of sliding mode control (SMC) and LQR for stabilization control of Quadcopter [1], combining SMC with variable weights and LQR for trajectory tracking control problem for dual-motor autonomous steering system [2], sliding mode - disturbance observer (SMC-DO) combines with LQR technique for controlling flexible manipulators robot [3], controlling 3D overhead crane systems by using PID-SMC [4], adaptive back-stepping sliding mode [5], optimum fuzzy combination of decoupled SMC (DSMC) [6], a feed-forward controller combines with feedback controller for tracking control problem [7], adaptive radical basis function neural networks associates with proportional derivative-SMC method [8], adaptive fuzzy logic back-stepping methodology [9], combination of state feedback controller with RBF [10], SMC integrates with partial feedback linearization for a spatial ballbot [11]. In addition, combination of control strategies for swing-up problem have been studied. For instance, research of combining two strategies consists of deep reinforcement learning and local control for swinging up acrobot [12], feedback linearization - energy control method combination for swing-up control of rotary inverted pendulum (RIP) [13], an experiment of combination of on-off and SMC methods for swinging up a pendulum with two reaction wheels [14], Q-learning and PID controllers combination for swinging up a nonlinear double inverted pendulum [15] and more.

In this work, we develop an IOFLALQR from IOFL method. The new suggested control algorithm is qualified to stabilize a fourth-order under-actuated nonlinear Furuta pendulum system. Furuta pendulum system, named after Japanese Professor Katsuhisa Furuta, was invented at Tokyo Institute of Technology. The first study was completed on this system in 1992 related to an application of pseudo-state feedback for swinging up an inverted pendulum [16]. Currently, Furuta pendulum or RIP, can find easily in laboratories related to control engineering. Furuta pendulum is single-input multi-output system (SIMO). In this paper, we validate the proposed control scheme on this Furuta pendulum system, which is available at Control System Laboratory, HCMUTE. Many researches have been done on this system such that back-stepping control scheme [17], LQR technique [18], SMC [19], IOFL [20], PID-Neural controller [21].

Feedback linearization consists of two control strategies: IOFL and exact state-space linearization. In this paper, we focus on input-output linearization approach. This method transforms a certain class of nonlinear systems into linear systems by a proper coordinate change and a linearizing state feedback [22]. Detail of this control scheme can be found in [23]. LQR is able to overcome big disturbance is going on stability the system without reducing working performance and can overcome disturbances that occurred previously [24].

Main contribution of this paper are proposed new technology, namely IOFLALQR. This control strategy is conducted on both simulation and experimental setup. After that, we compare the state responses of output system between IOFLALQR and LQR technique.

2. Furuta Pendulum System

2.1. Mathematical Model

Structure of RIP is shown in Fig. 1

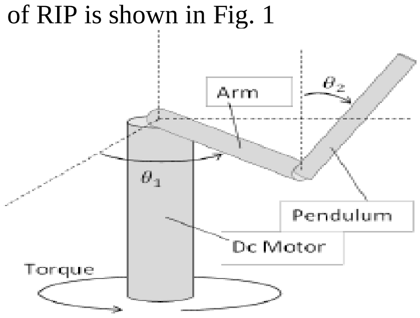

Fig. 1. RIP

Parameters of system are listed in Table 1. These parameters are measured from real model in Fig. 2.

Table 1. System parameters

Parameter	Value	Unit	Description
m	0.027	kg	Mass of pendulum
L_1	0.205	m	Length of arm
J_1	0.0019	kgm^2	Inertial moment of arm
L_2	0.328	m	Length of pendulum
J_2	0.0046617	kgm^2	Inertial moment of pendulum
C_1	0.025	N m s/rad	Friction coefficient of arm
C_2	0.0017	N m s/rad	Friction coefficient of pendulum
K_t	0.0531	Nm/A	Torque constant of DC motor
R_m	11.7356	Ω	Motor armature coil resistance
g	9.81	m/s^2	Gravitation acceleration
θ_1	na	rad	Angular position of arm
θ_2	na	rad	Angular position of pendulum
e	na	V	Control input

According to [25], equations of of RIP are presented:

$$M(\theta)\ddot{\theta} + C(\theta,\dot{\theta}) + G(\theta) = \begin{bmatrix} \tau & 0 \end{bmatrix}^T \quad (1)$$

where,

$$M(\theta) = \begin{bmatrix} J_1 + mL_1^2 + mL_2^2 \sin^2(\theta_2) & -mL_1L_2\cos(\theta_2) \\ -mL_1L_2\cos(\theta_2) & J_2 + mL_2^2 \end{bmatrix};$$

$$C(\theta,\dot{\theta}) = \begin{bmatrix} C_1 + \frac{1}{2} mL_2^2 \dot{\theta}_2 \sin 2\theta_2 & \begin{matrix} mL_1L_2\dot{\theta}_2 \sin\theta_2 + \\ + \frac{1}{2} mL_2^2 \dot{\theta}_1 \sin 2\theta_2 \end{matrix} \\ -\frac{1}{2} mL_2^2 \dot{\theta}_1 \sin 2\theta_2 & C_2 \end{bmatrix};$$

$$G(\theta) = \begin{bmatrix} 0 \\ mgL_2 \sin\theta_2 \end{bmatrix}$$

Relationship of output τ and voltage e is given by

$$\tau = -k_2\dot{\theta}_1 + k_1 e \quad (2)$$

where $k_1 = K_t / R_m$; $k_2 = K_t^2 / R_m$

The state-space equations of RIP are given below. Consider $x_1 = \theta_2$ as output of system. We obtain

$$\dot{x} = f(x) + g(x)e; \; y = h(x) \quad (3)$$

where $x = \begin{bmatrix} x_1 & \dot{x}_1 & x_2 & \dot{x}_2 \end{bmatrix}^T = \begin{bmatrix} \theta_2 & \dot{\theta}_2 & \theta_1 & \dot{\theta}_1 \end{bmatrix}^T$;

$$f(x) = \begin{bmatrix} 0 & f_1(x) & 0 & f_2(x) \end{bmatrix}^T;$$

$$g(x) = \begin{bmatrix} 0 & g_1(x) & 0 & g_2(x) \end{bmatrix}^T;$$

$$f_1(x) = \frac{mL_1L_2\cos x_1}{J_2 + mL_2^2} f_2(x) + \frac{1}{J_2 + mL_2^2}\left(\frac{1}{2} mL_2^2 x_4^2 \sin 2x_1 - C_2x_2 + mgL_2 \sin x_1\right);$$

$$g_1(x) = \frac{mL_1L_2\cos x_1}{J_2 + mL_2^2} g_2(x);$$

$$f_2(x) = \frac{\begin{bmatrix} -\left(\begin{matrix} C_1 + k_2 + \frac{1}{2} mL_2^2 x_2 \sin 2x_1 + \\ -\frac{m^2 L_1 L_2^2 x_4 \cos x_1 \sin 2x_1}{2\left(J_2 + mL_2^2\right)} \end{matrix}\right) x_4 + \\ -\left(\begin{matrix} mL_1L_2x_2 \sin x_1 + \frac{1}{2} mL_2^2 x_4 \sin 2x_1 + \\ + \frac{C_2 mL_1L_2x_2 \cos x_1}{J_2 + mL_2^2} \end{matrix}\right) x_2 + \\ + \frac{m^2 g L_1 L_2^2 \cos x_1 \sin x_1}{\left(J_2 + mL_2^2\right)} \end{bmatrix}}{J_1 + mL_1^2 + mL_2^2 \sin^2 x_1 - \frac{m^2 L_1^2 L_2^2 \cos^2 x_1}{J_2 + mL_2^2}};$$

$$g_2(x) = \frac{k_1}{J_1 + mL_1^2 + mL_2^2 \sin^2 x_1 - \frac{m^2 L_1^2 L_2^2 \cos^2 x_1}{J_2 + mL_2^2}}$$

Linearized system operating around the equilibrium point is described as follows:

$$\dot{x} = Ax + Be \tag{4}$$

where, $A = \begin{bmatrix} 0 & 1 & 0 & 0 \\ a_{21} & a_{22} & a_{23} & a_{24} \\ 0 & 0 & 0 & 1 \\ a_{41} & a_{42} & a_{43} & a_{44} \end{bmatrix}$; $B = \begin{bmatrix} 0 \\ b_2 \\ 0 \\ b_4 \end{bmatrix}$;

$$a_{21} = \frac{\partial \ddot{\theta}_2}{\partial x_1};\ a_{22} = \frac{\partial \ddot{\theta}_2}{\partial x_2};\ a_{23} = \frac{\partial \ddot{\theta}_2}{\partial x_3};\ a_{24} = \frac{\partial \ddot{\theta}_2}{\partial x_4};\ a_{41} = \frac{\partial \ddot{\theta}_1}{\partial x_1};$$

$$a_{42} = \frac{\partial \ddot{\theta}_1}{\partial x_2};\ a_{43} = \frac{\partial \ddot{\theta}_1}{\partial x_3};\ a_{44} = \frac{\partial \ddot{\theta}_1}{\partial x_4};\ b_2 = \frac{\partial \ddot{\theta}_2}{\partial e};\ b_4 = \frac{\partial \ddot{\theta}_1}{\partial e}$$

From [26], we analyze the stability of system. Let $x = 0$ be an equilibrium point of nonlinear system

$$x = f(x) \tag{5}$$

where $f : D \rightarrow \mathbb{R}^n$ is continuously differentiable and D is a neighborhood of the origin. Let

$$A = \left. \frac{\partial f(x)}{\partial x} \right|_{x=0} \tag{6}$$

1. The origin is asymptotically stable if $\operatorname{Re}\lambda_i < 0$ for all eigenvalues of *A*.
2. The origin is unstable if $\operatorname{Re}\lambda_i > 0$ for one or more of the eigenvalues of *A*.

Accordingly, considering the nonlinear RIP system (3). RIP has an equilibrium point $x = \begin{bmatrix} 0 & 0 & 0 & 0 \end{bmatrix}^T$. Now, we investigate the stability of this point using linearization. $rank\begin{bmatrix} B & AB \end{bmatrix} = 4$, it means that (*A*, *B*) is controllable. The eigenvalues of *A* are

$$\lambda_1 = 0;\ \lambda_2 = 5.6731;\ \lambda_3 = -6.7788;\ \lambda_4 = -1.8732 \tag{7}$$

With results in (7), there is one eigenvalue in the open right-half plane. Hence, the system is unstable at equilibrium point.

2.2. Experimental Setup

The real-time experimental setup is similar with the experimental setup [20].

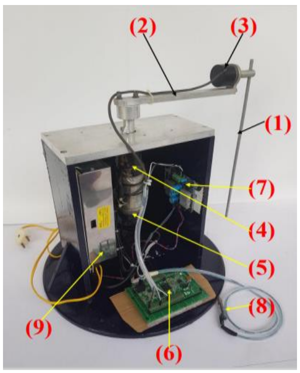

Fig. 2. Experimental setup

Components consist of:

1) Pendulum link
2) Arm link
3) Encoder of pendulum link (500 RPM)
4) DC motor TAMAGAWA SEIKI 24VDC - 30W
5) Encoder of arm link (100 RPM)
6) Micro-controller STM32F407VG Discovery board
7) Driver IR2184
8) Module UART CP2102
9) Power supplier 24VDC-10A

3. Methodology

3.1. IOFL

Principles of IOFL and application of IOFL for Furuta pendulum are mentioned in [20]. The calculation of control law bases on the state-space equation (3), which follows closely the designed controller in [20]. In this manuscript, we re-use the control law that mentioned in [20]. Schematic diagram of IOFL is shown in Fig. 3.

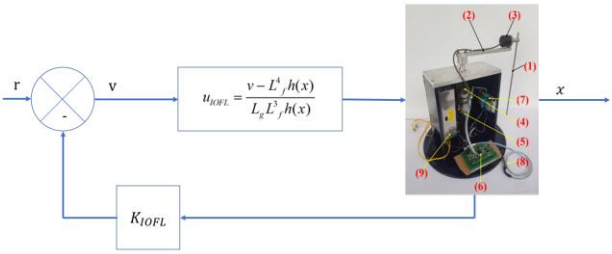

Fig. 3. IOFL control scheme

Control signal of this method is

$$u_{IOFL} = \frac{v - L^4{}_f h(x)}{L_g L^3{}_f h(x)} \tag{8}$$

where, $v = -K_{IOFL} z$; *K* is a positive matrix that need to be selected with *n* is a number of degrees of system; *z* is states vector: $z = \begin{bmatrix} z_1 & z_2 & z_3 & z_4 \end{bmatrix}$;

$z = \begin{bmatrix} h(x) & L_f h(x) & L_f^2 h(x) & L_f^3 h(x) \end{bmatrix}$; $h = x_1$;

$f = \begin{bmatrix} x_2 & f_1(x) & x_4 & f_2(x) \end{bmatrix}^T$;

$g = [0 \quad g_1(x) \quad 0 \quad g_2(x)]^T$;

$$L_f h = \begin{bmatrix} \frac{\partial h}{\partial x_1} & \frac{\partial h}{\partial x_2} & \frac{\partial h}{\partial x_3} & \frac{\partial h}{\partial x_4} \end{bmatrix} f;$$

$$L^2{}_f h = \begin{bmatrix} \frac{\partial L_f h}{\partial x_1} & \frac{\partial L_f h}{\partial x_2} & \frac{\partial L_f h}{\partial x_3} & \frac{\partial L_f h}{\partial x_4} \end{bmatrix} f;$$

$$L^3{}_f h = \begin{bmatrix} \frac{\partial L_f^2 h}{\partial x_1} & \frac{\partial L_f^2 h}{\partial x_2} & \frac{\partial L_f^2 h}{\partial x_3} & \frac{\partial L_f^2 h}{\partial x_4} \end{bmatrix} f;$$

$$L^4{}_f h = \begin{bmatrix} \frac{\partial L_f^3 h}{\partial x_1} & \frac{\partial L_f^3 h}{\partial x_2} & \frac{\partial L_f^3 h}{\partial x_3} & \frac{\partial L_f^3 h}{\partial x_4} \end{bmatrix} f$$

In addition, by using genetic algorithm (GA), the controlled parameters $K_{IOFL} = [K_1 \quad K_2 \quad K_3 \quad K_4]$ are determined as follows:

$$K_1 = 0.01;\ K_2 = 82;\ K_3 = 45.41;\ K_4 = 1.41 \tag{9}$$

3.2. LQR

LQR controller is widely used in control engineering for stabilization control under-actuated system like inverted pendulum, pendubot, etc. General control law of LQR technique is

$$u_{LQR} = -K_{LQR}x \tag{10}$$

where, $K_{LQR} = [129.6261 \quad 23.8921 \quad -5 \quad -6.0310]$ is calculated from weighing matrixes Q, R from GA searching, linear matrices A, B from (4) and system parameters in Table 1. These matrices are listed as below

$$A = \begin{bmatrix} 0 & 1 & 0 & 0 \\ 36.4628 & -0.0392 & 0 & -1.5058 \\ 0 & 0 & 0 & 1 \\ 23.3433 & -0.0251 & 0 & -2.9396 \end{bmatrix};\ B = \begin{bmatrix} 0 \\ 1.1365 \\ 0 \\ 2.2186 \end{bmatrix};$$
$$Q = \begin{bmatrix} 1 & 0 & 0 & 0 \\ 0 & 0 & 0 & 0 \\ 0 & 0 & 10 & 0 \\ 0 & 0 & 0 & 0 \end{bmatrix};\ R = 0.4 \tag{11}$$

3.3. IOFLALQR

The advantage of LQR is simple structure and well-stabilizing RIP around working point. However, the working space is just being around the working point. Differently, nonlinear control, such as IOFL method, has wide range of working due to flexible structure of controller and stability proved from Lyapunov criteria. Disadvantage of IOFL method is the difficulty in selecting function *h(x)* in (8). With the selection of $h(x)=x_1$, only the angle of pendulum is guaranteed. The motion of arm is not kept closed to zero value. Following to [20], the arm cannot be kept closed to zero point. It moves around the working point, about 20 degrees with sine form. Then, we propose a hybrid controller which can combine LQR and IOFL to stabilize RIP at working point as in Fig. 4.

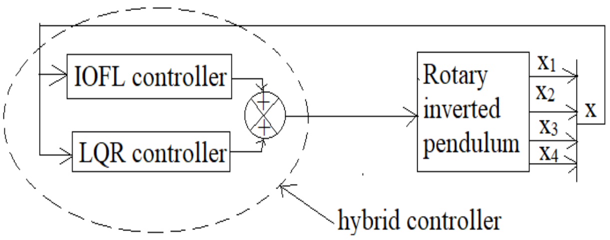

Fig. 4. Hybrid controller in controlling RIP

The introduced RIP controller is based on a combination of input-output feedback linearization (IOFL) and linear quadratic regulator (LQR). Simulink schematic of representation of IOFLALQR method is drawn in Fig. 5.

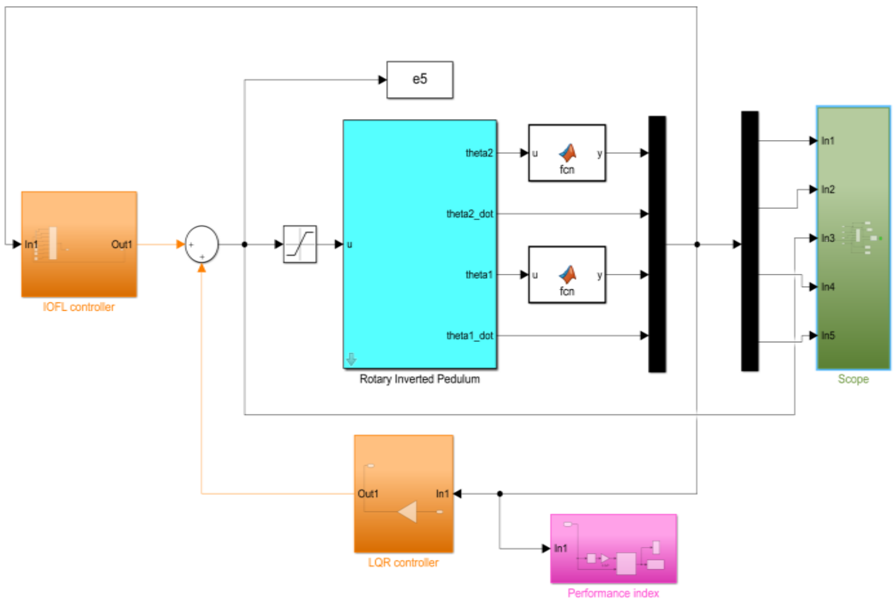

Fig. 5. Simulink model of IOFLALQR in controlling RIP

4. Validation

4.1. Numerical Simulation Results

In this subsection, simulation results are shown in Fig. 6 and Fig. 7. Content of Fig. 6 is performance of state responses of output system by implementing IOFLALQR. In Fig. 6, from top to bottom, graphs are organized as follows: state response of angular position of pendulum θ_2 (rad), state response of angular velocity of pendulum $\dot{\theta}_2$ (rad/s), state response of angular position of pendulum θ_1 (rad), state response of angular velocity of pendulum $\dot{\theta}_1$ (rad/s), control input (V). Besides, the simulation results compare the state responses of RIP on θ_2, $\dot{\theta}_2$, θ_1, $\dot{\theta}_1$, and control input, respectively is shown in Fig. 7. State responses of system under IOFLALQR are described in blue and state responses of system under LQR are described in orange. Original points are set up for this simulation as follows: $x = \begin{bmatrix} 0.1 & 0 & 0.1 & 0 \end{bmatrix}^T$ (rad).

Following first graph of Fig. 7, angle of pendulum is back to equilibrium point after 2 seconds, maximum overshot range of this state is *[-0.03;0.1]* (rad). In third graph, angle of arm stabilizes at "0" (rad) after 4 seconds and maximum overshoot range of this state is *[-0.3;0.1]* (rad). Angular velocity of pendulum and arm are depicted in 2nd and 4th graph of this figure. We can observe that system under IOFLALQR can stabilize at equilibrium point. Moreover, control input of RIP is described in 5th graph.

Moreover, from Fig. 7, system with LQR controller has more significant overshoots in angular displacements of pendulum and arm. From simulation results, it can be observed that system with IOFLALQR has better performance, in terms of less overshoot, faster convergence in pendulum angle, and arm angle. In addition, control input of two controllers are also compared in last graph of Fig. 7.

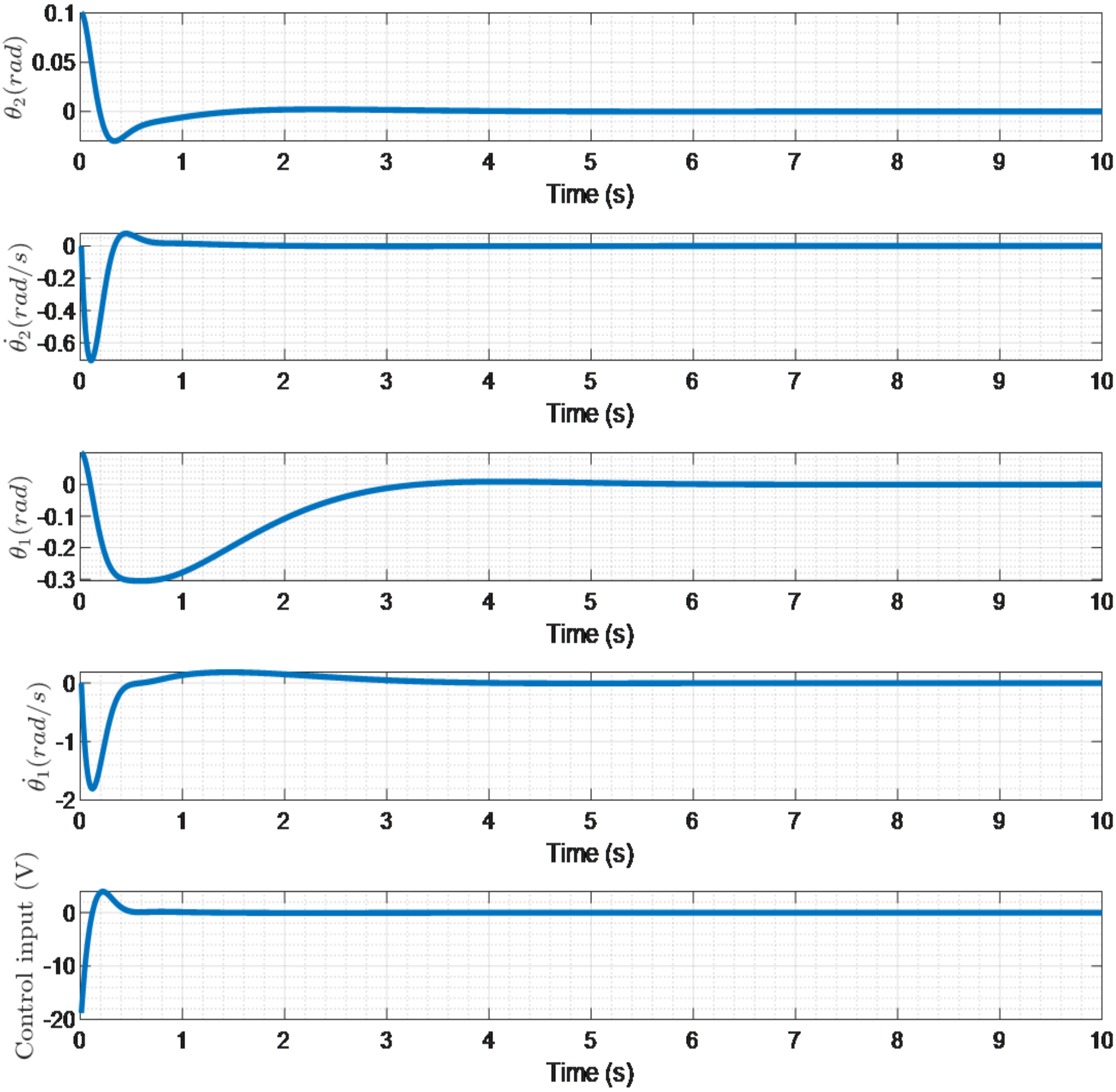

Fig. 6. State responses of output system under IOFLALQR method

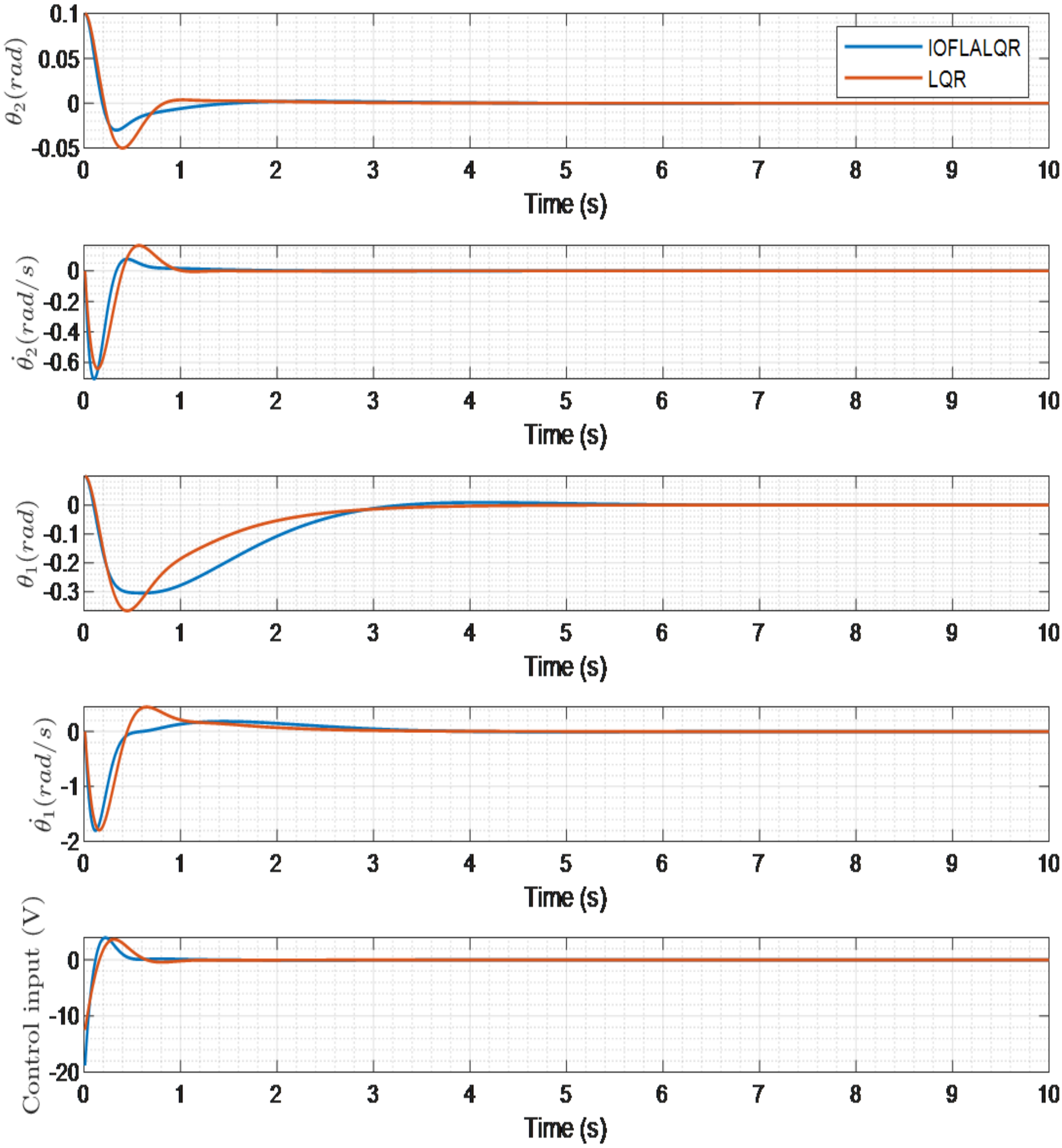

Fig. 7. Comparison of state responses of output system under IOFLALQR and LQR techniques

4.2. Experimental Results

The main purpose of this subsection is to provide performance of RIP via experiment. Experiment results are drawn in Fig. 8. Contents of Fig. 8 are performance of state responses of output system by implementing IOFLALQR and conventional LQR techniques. In Fig. 8, from the top to bottom, graphs are organized as follows: state response of angular position of pendulum θ_2 (rad), state response of angular velocity of pendulum $\dot{\theta}_2$ (rad/s), state response of angular position of pendulum θ_1 (rad), state response of angular velocity of pendulum $\dot{\theta}_1$ (rad/s), control input (V). State responses of system under IOFLALQR are described in blue and state responses of system under LQR are described in orange. Following the first and third graph, pendulum angle has a minor oscillation around equilibrium point and better performance than another, while the angle of arm of system with IOFLALQR has better performance than conventional LQR. The angular velocity of arm and pendulum of system with IOFLALQR and conventional LQR are also captured in the 2nd and 4th graph of this figure. The comparison of voltage input is also provided in the last graph of Fig. 8.

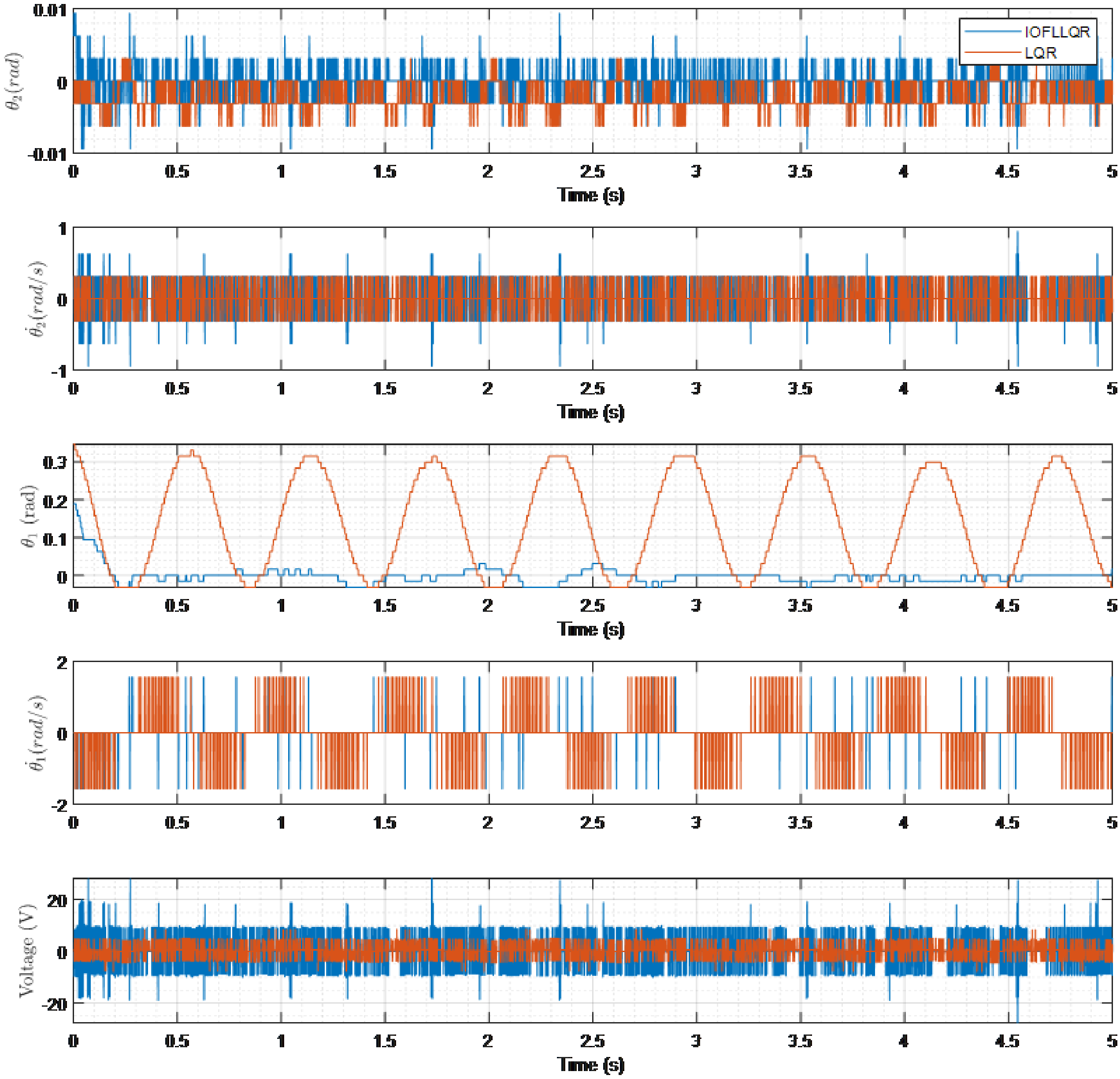

Fig. 8. Comparison of state responses of output system with IOFLALQR and LQR techniques

5. Conclusion

The purpose of this paper is to qualify the proposed stabilization control of nonlinear RIP system, namely IOFLALQR. The stabilizing control laws of RIP were designed, realized, and experimentally tested. IOFLALQR was designed based on combination of input-output feedback linearization (IOFL) and linear quadratic regulator (LQR). The results showed that the proposed control law guarantees the closed-loop system to be asymptotically stable. The experimental setup was built, and the controllers were realized. The designed control system demonstrated to be effective in simulation and experimental results. In the simulation studies, IOFLALQR control scheme yields a smaller pendulum angle deviation, a smaller arm angle deviation, and a smaller angular velocity of arm and pendulum deviation than conventional LQR. In the experimental work, IOFLALQR was applied successfully on physical experimental RIP. The future work can be realized such as validation of IOFLALQR on other under-actuated system like inverted pendulum, etc.

Acknowledgement

This work belongs to project T2023-44 which is funded by Ho Chi Minh city University of Technology and Education (HCMUTE), Vietnam, for year 2023. We, authors, appreciate this support.

6. References

[1] Ahmet K., R. Elagib: "Implementation and Stabilization of a Quadcopter Using Arduino and the Combination of LQR and SMC Methods", Journal of Engineering Research and Reports, vol. 23, no. 7, pp. 42-58, 2022.
[2] Zhongwei W., Xu X., Xie J., Liu Z., He S.: "Trajectory tracking control considering the transmission backlash of the dual-motor autonomous steering system", Proceedings of the Institution of Mechanical Engineers, Part D: Journal of Automobile Engineering, p. 09544070231161845, 2023.
[3] Xu Y., Dou K., Wang L., Yang C., Wang K.: "Composite control of flexible manipulators based on SMC-DO and LQR", in 2020 Chinese Control And Decision Conference (CCDC), Hefei, China, 2020.
[4] Wang S., Jin W.: "A PID-SMC control method with payload anti-swing for 3D overhead crane systems", in 2022 34th Chinese Control and Decision Conference (CCDC), Hefei, China, 2022.
[5] Zhao Y., Sun X., Wang G., Fan Y.: "Adaptive Backstepping Sliding Mode Tracking Control for Underactuated Unmanned Surface Vehicle With Disturbances and Input Saturation", IEEE Access, vol. 9, pp. 1304-1312, 2021.
[6] Mahmoodabadi M.J., Soleymani T.: "Optimum fuzzy combination of robust decoupled sliding mode and adaptive feedback linearization controllers for uncertain under-actuated nonlinear systems", Chinese Journal of Physics, vol. 64, pp. 241-250, 2020.
[7] Berger T., Drücker S., Lanza L., Reis T., Seifried R.: "Tracking control for underactuated non-minimum phase multibody systems", Nonlinear Dynamics, vol. 104, p. 3671–3699, 2021.
[8] Zhi L., Xin M., Yibin L.: "Robust tracking control strategy for a quadrotor using RPD-SMC and RISE", Neurocomputing, vol. 331, pp. 312-322, 2019.
[9] Naige W., Cao G.: "Adaptive fuzzy backstepping control of underactuated multi-cable parallel suspension system with tension constraint", ransactions of the Institute of Measurement and Control , vol. 43, no. 9, pp. 1971-1984, 2021.
[10] Mohammed M.: "Nonlinear state feedback controller combined with RBF for nonlinear underactuated overhead crane system", Journal of Engineering Research, vol. 9, no. 3A, 2021.
[11] Ba P.D., Kim J., Lee S.G.: "Combined control with sliding mode and partial feedback linearization for a spatial ridable ballbot", Mechanical Systems and Signal Processing, vol. 128, pp. 531-550, 2019.
[12] Gillen S., Molnar M., Byl K.: "Combining Deep Reinforcement Learning And Local Control For The Acrobot Swing-up And Balance Task", in 2020 59th IEEE Conference on Decision and Control (CDC), Jeju, Korea (South), 2020.
[13] Nguyen N.P., Oh H., Kim Y., Moon J.: "A nonlinear hybrid controller for swinging-up and stabilizing the rotary inverted pendulum," Nonlinear Dynamics, vol. 104, p. 1117–1137 , 2021.
[14] Trentin J.F.S., Da Silva S., De S. Ribeiro J.M., Schaub H.: "An experimental study to swing up and control a pendulum with two reaction wheels", Meccanica, vol. 56, p. 981–990, 2021.
[15] Zeynivand A., Moodi H.: "Swing-up Control of a Double Inverted Pendulum by Combination of Q-Learning and PID Algorithms", in 2022 8th International Conference on Control, Instrumentation and Automation (ICCIA), Tehran, Iran, Islamic Republic of, 2022.
[16] Katsuhisa F., Yamakita M., Kobayashi S.: "Swing-up control of inverted pendulum using pseudo-state feedback", Proceedings of the Institution of Mechanical Engineers, Part I: Journal of Systems and Control Engineering, vol. 206, no. 2, pp. 263-269, 1992.
[17] Vo M.T., et al.: "Back-stepping control for rotary inverted pendulum," JTE, vol. 59, p. 93–101, 2020.
[18] Vo A.K., Nguyen M.T., Tran V.D., Nguyen T.V., Nguyen V.D.H.: "Model and control algorithm construction for rotary inverted pendulum in laboratory", JTE, vol. 49, p. 32–40, 2018.
[19] Le Q.V., Nguyen M.T., Duong H.N.: "Sliding mode control for rotary inverted pendulum", JTE, vol. 34, p. 24–29, 2015.
[20] Vo M.T.: "Design of Input-Output Feedback Linearization Control for Rotary Inverted Pendulum System", JTE, vol. 69, p. 26–35, Apr. 2022.
[21] Nguyễn V.Đ.H., Ngô V.T.: "PID-neuron controller design for rotary inverted pendulum system", JTE, vol. 23, p. 37–43, 2012.
[22] Kumar A.A., Antoine J.F., Abba G.: "Input-Output Feedback Linearization for the Control of a 4 Cable-Driven Parallel Robot", IFAC-PapersOnLine, vol. 52, no. 13, pp. 707-712, 2019.
[23] Nghia D.H., Hệ Đ.K., Biến T.Đ.: TPHCM: vnuhcmpress, 2011.
[24] Heri P., Purwanto E.B.: "Design of linear quadratic regulator (LQR) control system for flight stability of LSU-05", Journal of Physics: Conference Series, vol. 890, no. 1, 2017.
[25] Yang X., Zheng X.: "Swing-Up and Stabilization Control Design for an Underactuated Rotary Inverted Pendulum System: Theory and Experiments", IEEE Transactions on Industrial Electronics, vol. 65, no. 9, pp. 7229-7238, 2018.
[26] Khalil H.K.: "Lyapunov Stability", Nonlinear Systems, Upper Saddle River. New Jersey 07458, Prentice-Hall. Inc, pp. 120-132, 1996.